IOP Conf. Series: Materials Science and Engineering **140** (2016) 012005 doi:10.1088/1757-899X/140/1/012005

The effect of hydrogen on strain hardening and fracture mechanism of high-nitrogen austenitic steel

G G Maier[1], E G Astafurova[1], E V Melnikov[1], V A Moskvina[2], V F Vojtsik[2], N K Galchenko[1] and G N Zakharov[3]
[1]Institute of Strength Physics and Materials Science, Siberian Branch of Russian Academy of Sciences, Akademichesky Avenue 2/4, Tomsk, 634055, Russia
[2]National Research Tomsk Polytechnic University, Lenina Avenue 30, Tomsk, 634050, Russia
[3]National Research Tomsk State University, Lenina Avenue 36, Tomsk, 634050, Russia

E-mail: elena.g.astafurova@gmail.com

Abstract. High-nitrogen austenitic steels are perspective materials for an electron-beam welding and for producing of wear-resistant coatings, which can be used for application in aggressive atmospheres. The tensile behavior and fracture mechanism of high-nitrogen austenitic steel Fe-20Cr-22Mn-1.5V-0.2C-0.6N (in wt.%) after electrochemical hydrogen charging for 2, 10 and 40 hours have been investigated. Hydrogenation of steel provides a loss of yield strength, uniform elongation and tensile strength. The degradation of tensile properties becomes stronger with increase in charging duration – it occurs more intensive in specimens hydrogenated for 40 hours as compared to ones charged for 2–10 hours. Fracture analysis reveals a hydrogen-induced formation of brittle surface layers up to 6 μm thick after 40 hours of saturation. Hydrogenation changes fracture mode of steel from mixed intergranular-transgranular to mainly transgranular one.

1. Introduction

Austenitic stainless steels are frequently used materials for industrial applications due to their high ductility at cryogenic temperatures and low aggressive environment embrittlement. It concerns mainly AISI 300-series Cr-Ni steels [1-3]. However, the presence of expensive alloying elements – nickel – and low yield stresses limit their use. The requirements of low costs have generated an interest in replacement of nickel and use nitrogen and manganese as alloying elements. The high-nitrogen Cr-Mn steels have good mechanical properties and corrosion resistance and could be of great interest for a wide range of industrial application – in particular, for producing wear-resistant coatings or items using electron-beam welding [4] or other methods of additive technologies. An indubitable advantage of such materials could be their good strength to wear combined with resistivity to degradation in aggressive atmospheres, for instance, in hydrogen.

Hydrogen embrittlement behavior of high-nitrogen steel is defined by the complex of several parameters; among them are stacking fault energy (SFE), steel composition, regime of hydrogenation and hydrogen content. Michler et al. [5] demonstrated that replacement of Ni on Mn and N of Cr-Mn austenitic steel decrease the resistance to hydrogen embrittlement. Authors [6] reported that amount

of nitrogen in solid solution of Cr-Mn steel had strong effect on its ductility under hydrogen charging: specimens with highest nitrogen content (0.6N, wt.%) dissolved more hydrogen and had a higher loss in ductility in comparison with 0.3N wt.% specimens. At the same time, Stoltz and co-authors [7] demonstrated that nitrogen in Cr-Ni-Mn-N steel lowered the SFE value until the N concentration reached 0.24 wt.%, but further increase in nitrogen content up to 0.52 wt.% did not change the value of SFE. Michler et al. [8] also found that SFE, as well as martensitic transformations, did not directly control the susceptibility to hydrogen-enhanced embrittlement of austenitic steels, but initial deformation mode was one important parameter respected for tensile ductility in hydrogen atmosphere. Igata et al. [9] investigated dislocation structure and ductility of Fe-Cr-Ni-Mn-0.35N, wt.% austenitic steel after hydrogenation. They reported that hydrogen decreased SFE, suppressed cross slip, decreased the dislocation multiplication rate and made ductility lower [9]. The effect of hydrogen on the properties of high-nitrogen steels was not studied in detail, and the problem of hydrogen environment embrittlement is still far from a final decision.

The present study tried to shed light on tensile behavior and fracture mechanism of high-nitrogen austenitic steel after hydrogenation.

2. Materials and methods

A high-nitrogen Fe-20Cr-22Mn-1.5V-0.2C-0.6N, wt. % steel was selected as an object of investigation. Steel specimens were quenched after 1100°C, 1 h. into cold water.

Before hydrogenation the specimen were cut dog-bone shaped flat tensile specimens with nominal dimensions of 18 mm x 2.7 mm x 0.7 mm (thickness) in the gauge section. Mechanical grinding and a final electrochemical polishing (50 g CrO_3, in 200 g H_3PO_4) were employed to remove the entire processing-affected surface layer. The final thickness of tensile specimens was 0.5 mm.

Electrochemical hydrogen charging was performed at current density of 50 mA/cm^2 for t_{hyd} = 2, 10, 40 hours at room temperature in 1M H_2SO_4 water solution, containing 0.25g l^{-1} of CH_4N_2S as a recombination poison. After hydrogenation, the tensile tests were conducted at room temperature and a strain rate of 5.6×10^{-4} s^{-1} using Instron 3369 electromechanical machine.

The fracture and side surface of specimens were examined using a LEO EVO 50 (Zeiss, Germany) scanning electron microscope (SEM).

3. Results and discussion

Figure 1 shows the tensile stress-strain curves for hydrogen-free and hydrogen-charged specimens. The detailed results of tensile tests are summarized in Table 1.

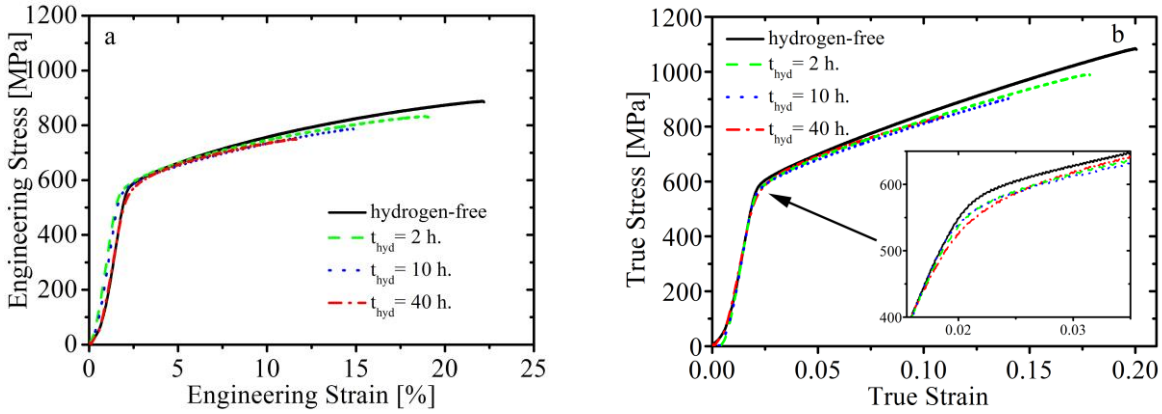

Figure 1. Stress-strain curves depending on hydrogenation duration: (a) engineering stress versus engineering strain; (b) true stress versus true strain.

Table 1. Influence of hydrogenation regime on yield stress ($\sigma_{0.2}$), uniform elongation (ε_{un}), tensile strength (σ_B), strain-hardening coefficient $\theta = (\sigma_{un} - \sigma_0)/(\varepsilon_{un} - \varepsilon_0)$ and hydrogen embrittlement index (E_H) according to true stress-true strain curves.

Treatment	$\sigma_{0.2}$ (MPa)	ε_{un} (%)	σ_B (MPa)	Θ (MPa)	E_H (%)
Hydrogen-free	586	20	1084	2800	0
t_{hyd} = 2 h.	538	17	989	2770	15
t_{hyd} = 10 h.	541	14	902	2780	30
t_{hyd} = 40 h.	520	11	838	3140	45

Increase in hydrogenation duration slightly decreases a yield stress of steel: from 586 MPa in hydrogen-free down to 520 MPa in hydrogen-charged specimens (for 40 h.). The elongation deteriorates under hydrogen saturation from 20 % for hydrogen-free specimens to 17 %, 14% and 11% after hydrogen charging for 2, 10 and 40 hours respectively. The hydrogen embrittlement index (E_H), representative of % loss in uniform elongation due to hydrogen alloying, was calculated using the following equation (Table 1):

$$E_H = [(\varepsilon_{un0} - \varepsilon_{unH})/\varepsilon_{un0}] \cdot 100\%,$$

where ε_{un0} and ε_{unH} are values of uniform elongation for hydrogen-free and hydrogen-charged specimens respectively. Analysis of data in table 1 shows that if the duration of hydrogenation reaches 40 hours, there is a maximum loss of uniform elongation and the highest value of E_H (45%) is observed. At the same time, the value of strain hardening coefficient does not change sufficiently with increasing of hydrogenation duration.

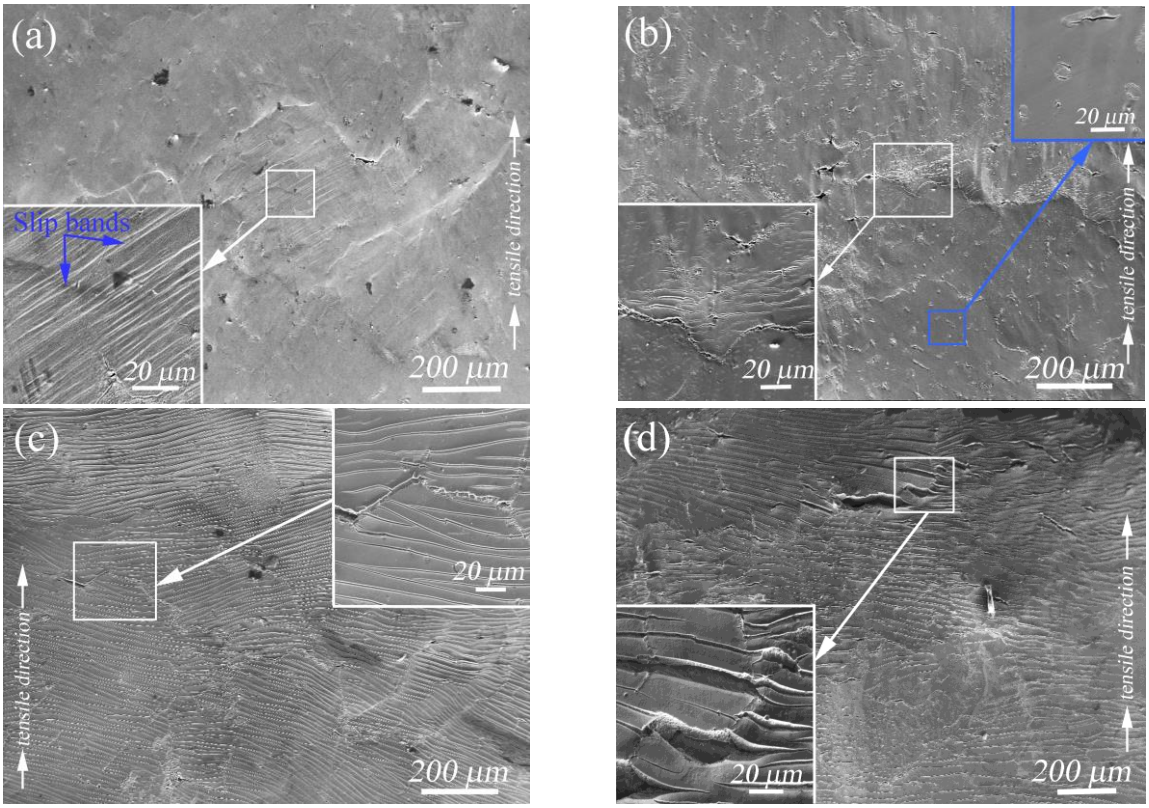

Figure 2. SEM micrographs of side surfaces of specimens without hydrogenation (a); after hydrogenation for 2 h. (b); after hydrogenation for 10 h. (c); after hydrogenation for 40 h. (d).

The micrographs of the side surfaces of specimens in initial state and after hydrogenation are presented in figure 2. The hydrogen-free specimen demonstrated slip bands inside of grains with the step of about 3 μm (Figure 2a). After 2 hours of hydrogen charging and tension, hydrogen-induced cracks are observed along grain boundaries and inside of them (Figure 2b). Some of these cracks with a length of 5-20 μm are detected inside of grains; other long cracks propagates through the grains perpendicular to tensile direction and have distance of 4 μm between them (Figure 2b, inserts). The micrographs clearly show that an increase in hydrogenation duration increases the distance between cracks and their depth: to 12 μm after 10 hours and to 17 μm after 40 hours of hydrogen saturation (Figures 2c-d). These differences in distance between cracks and crack depth are associated with the different thickness of hardened (brittle) layer and with different tensile elongation of specimens to fracture (Table 1).

The fracture surfaces of all specimens were examined to observe the influence of hydrogen on fracture behavior of the high-nitrogen steel (Figure 3). The hydrogen-free specimens were found to exhibit a predominantly intergranular ductile fracture (Figure 3a), but regions with transgranular fracture was also observed. A main feature of the fracture surface of hydrogen charged samples in comparison with hydrogen-free one is an appearance of brittle surface layer on the specimen surface (Figures 3 b-d). In the central area, the fracture morphology of the hydrogen-charged specimens is ductile. It contains regions with coarse dimples and fine dimples with parallel edges closely spaced to each others. Rough secondary macrocracks is observed in central part of hydrogenated specimens.

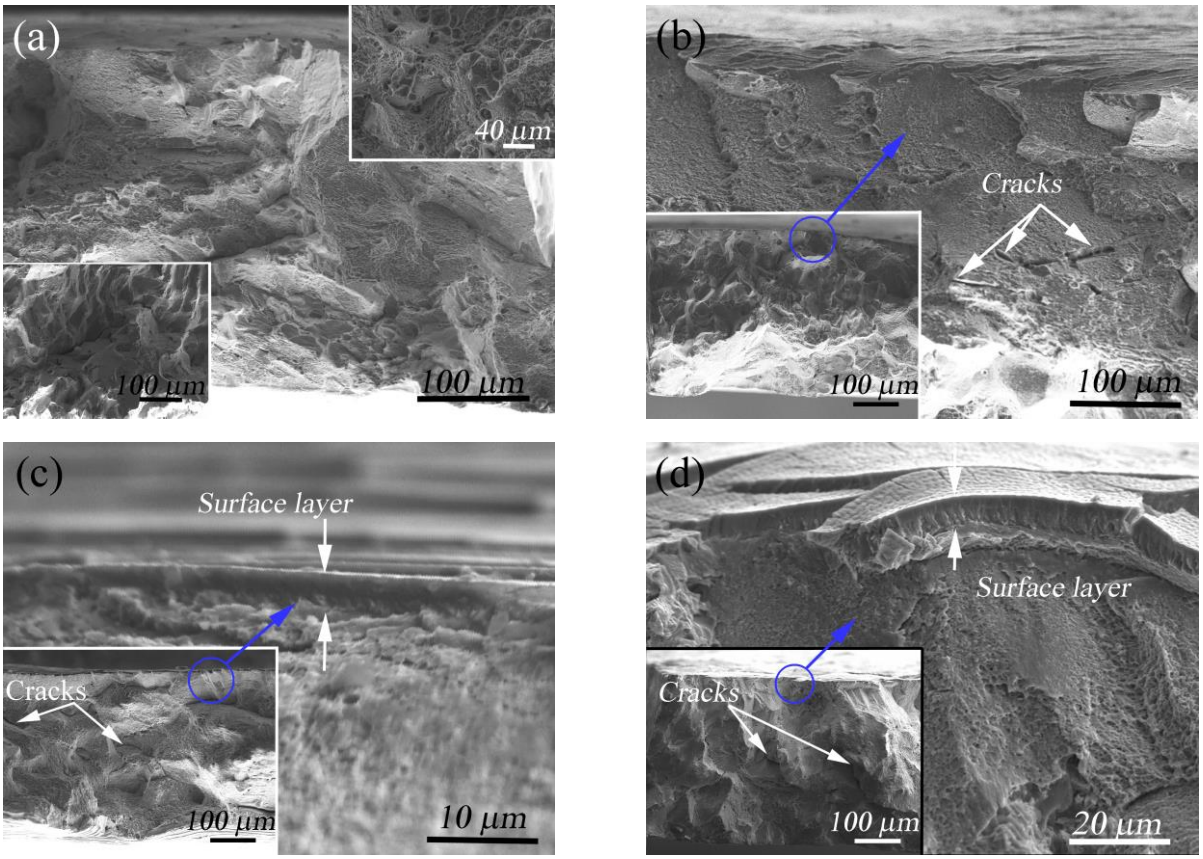

Figure 3. SEM micrographs of the fracture surfaces of hydrogen-free (a) and hydrogen-charged for 2h. (b), 10 h. (c), 40 h. (d) specimens.

The thin surface layer with the mean thickness of 1.5 μm forms after 2 h. hydrogenation of steel (Figure 3 b). The hydrogenation for 10 and 40 hours provides thicker brittle surface layers with a

thickness of 3.5 μm and 6 μm respectively (Figure 3 c, d). The hydrogen-assisted surfaces layers consist of two regions: the first one (surface) is homogeneous and brittle (cleavage-like); the second one (subsurface) characterized by columnar structure with the elongated dimples oriented perpendicular to surface. The fracture mode in hydrogen charged specimens is also mixed, but predominantly transgranular with parallel elongated dimples in different directions. The fracture character of the specimens after hydrogenation for 40 hours does not significantly change in comparison with the specimens charged for 10 hours (Figures 3 c-d). The embrittlement of a surface layer and nucleation of secondary macrocracks and microcracks in central ductile part of the hydrogenated steel specimens provoke their fast failure compared to hydrogen-free one.

The results clearly show that hydrogen charging changes fracture regime of high-nitrogen steel and provides the significant loss in uniform elongation of specimens. The change in fracture regime and appearance of parallel elongated dimples is connected with the fact that hydrogen reduces stacking fault energy of austenite, enhances slip localization and increases the nucleation of voids at the intersection of slip bands. Since deformation bands are usually planar, have regular spacing and intersect along lines, such nucleating voids appear as parallel elongated dimples. Similar feature was demonstrated for Cr-Ni austenitic steels by Nibur et al. [10]. Michler et al. [8] reported that high concentration of interstitial atoms in steel can influence the deformation mode not only via SFE but also by effects like short-range ordering and microtwinning. These effects, obviously, could arise in our case due to high concentration of nitrogen in solid solution and pronounced mechanical twinning in high-nitrogen steels [11]. The observed cracks in hydrogen-charged specimens can be also attributed to the hydrogen-enhanced localized plasticity [12] in austenite. Another possible explanation of change of fracture mode and appearance of cracks in hydrogen-charged specimens connected with two-phase composition (austenite and small portion of ferrite) of steel investigated. The diffusivity of hydrogen in ferrite higher than in austenite at room temperature [13], that could provoke an earlier fracture in ferrite phase compared to austenite one. The hydrogen can assisted fracture due to accumulation of hydrogen in ferrite-austenite interfaces and leads to embrittlement of structure. Obtained experimental results tend to support all presented explanations and required further detailed investigation of the steel structure.

4. Summary

The effect of hydrogen on tensile properties and fracture behavior of austenitic steel Fe-20Cr-22Mn-1.5V-0.2C-0.6N (in wt.%) has been investigated. Hydrogen decreases yield strength, uniform elongation and tensile strength of steel with increasing of hydrogenation duration. The formation of brittle surface layers occurs under hydrogenation, the mean thicknesses of these layers depends on charging regime and reaches 6 μm after hydrogenation for 40 hours. Surface layers crack under tension in cleavage-like manner. Analysis of fracture revealed that hydrogenation leads to change in fracture mode from mixed intergranular-transgranular to mainly transgranular one and promoted secondary cracking inside of specimens.

Acknowledgments

This research was partly supported by Russian Foundation for Basic Researches (project No. 15-38-20056, in part of mechanical characterization) and Russian President Scholarship (SP-160.2016.1, in part of electron microscopy). The experimental results were obtained using equipment of Center «Nanotech» of Institute of Strength Physics and Materials Science, Siberian Branch of Russian Academy of Sciences.

References

[1] Michler T, Naumann J, Hock M, Berreth K, Balogh M P, Sattler E 2015 *Mat. Sci. and Eng. A* **628** 252–61

[2] San Marchi C, Michler T, Nibur K A and Somerday B P 2010 *Int. J. Hydrogen Energy* **35 (18)** 9736–45
[3] Zhang L, Wen M, Imade M, Fukuyama S and Yokogawa K 2008 *Acta Mater.* **56 (14)** 3414–21
[4] Narkevich N A, Durakov V G , Tagiltseva D N, Shulepov A I and Smirnov A I 2013 *Phys. Met. Metall.* 2013 **114(6)** 535-44
[5] Michler T, Naumann J 2010 *Int. J. of Hydrogen Energy 35* 1485–92
[6] Phaniraj M P, Kim H-J, Suh J-Y, Shim J-H, Park S-J and Lee T-H 2015 *Int. J. of Hydrogen Energy* **40** 13635–42
[7] Stoltz R E and Vandersande J B *Metall. Trans A* 1980 **11A** 1033–37
[8] Michler T, San Marchi C., Naumann J, Weber S, Martin M 2012 *Int. J. of Hydrogen Energy* **37** 16231–46
[9] Igata N, Fujiga T and Yumoto H 1991 *J. Nucl. Mater.* **179** 656-58
[10] Nibur K A, Somerday B P, Balch D K, Marchi C S 2009 *Acta Mater.* **57** 3795–3809
[11] Gavrilyuk V G, Berns H 1999 High nitrogen steel Berlin (Springer Verlag Publ.) p 378
[12] Birnbaum H K and Sofronis P 1994 Mat. Sci. and Eng. A **176** 191–202
[13] Younes C M, Steele A M, Nicholson J A and Barnett C 2013 Int. J. Hydrogen Energy 38 4864–76